

RESEARCH ARTICLE

Past, present and future distributions of Oriental beech (*Fagus orientalis*) under climate change projections

Dilsad Dagtekin¹✉*, Evrim A. Şahan¹✉, Thomas Denk²‡, Nesibe Köse³‡, H. Nüzhet Dalfes¹‡

1 Eurasia Institute of Earth Sciences, Istanbul Technical University, Istanbul, Turkey, **2** Department of Paleobiology, Swedish Museum of Natural History, Stockholm, Sweden, **3** Department of Forest Botany, Faculty of Forestry, Istanbul University-Cerrahpasa, Istanbul, Turkey

✉ These authors contributed equally to this work.

✉ Current address: Department of Evolutionary Biology and Environmental Studies, University of Zurich, Zurich, Switzerland

‡ These authors also contributed equally to this work.

* dilsad.dagtekin@ieu.uzh.ch



OPEN ACCESS

Citation: Dagtekin D, Şahan EA, Denk T, Köse N, Dalfes HN (2020) Past, present and future distributions of Oriental beech (*Fagus orientalis*) under climate change projections. PLoS ONE 15 (11): e0242280. <https://doi.org/10.1371/journal.pone.0242280>

Editor: Michal Bosela, Technical University in Zvolen, SLOVAKIA

Received: June 9, 2020

Accepted: October 29, 2020

Published: November 17, 2020

Copyright: © 2020 Dagtekin et al. This is an open access article distributed under the terms of the [Creative Commons Attribution License](https://creativecommons.org/licenses/by/4.0/), which permits unrestricted use, distribution, and reproduction in any medium, provided the original author and source are credited.

Data Availability Statement: Part of our data is open-source and available to everyone online (<http://www.euforgen.org/species/fagus-orientalis/>), and part of our data belongs to the General Directory of Forestry, Turkey. That is why, we are not allowed to distribute the data ourselves, yet, it is available upon request to the General Directory of Forestry, Turkey. Here is the contact information: Republic of Turkey, General Directorate of Forestry Address: Beştepe Mahallesi Söğütözü Caddesi No:8/1 06560 Yenimahalle / ANKARA / TURKEY Phone: +90 312 296 40 00

Abstract

Species distribution models can help predicting range shifts under climate change. The aim of this study is to investigate the late Quaternary distribution of Oriental beech (*Fagus orientalis*) and to project future distribution ranges under different climate change scenarios using a combined palaeobotanical, phylogeographic, and modelling approach. Five species distribution modelling algorithms under the R-package ‘biomod2’ were applied to occurrence data of *Fagus orientalis* to predict distributions under present, past (Last Glacial Maximum, 21 ka, Mid-Holocene, 6 ka), and future climatic conditions with different scenarios obtained from MIROC-ESM and CCSM4 global climate models. Distribution models were compared to palaeobotanical and phylogeographic evidence. Pollen data indicate northern Turkey and the western Caucasus as refugia for Oriental beech during the Last Glacial Maximum. Although pollen records are missing, molecular data point to Last Glacial Maximum refugia in northern Iran. For the mid-Holocene, pollen data support the presence of beech in the study region. Species distribution models predicted present and Last Glacial Maximum distribution of *Fagus orientalis* moderately well yet underestimated mid-Holocene ranges. Future projections under various climate scenarios indicate northern Iran and the Caucasus region as major refugia for Oriental beech. Combining palaeobotanical, phylogeographic and modelling approaches is useful when making projections about distributions of plants. Palaeobotanical and molecular evidence reject some of the model projections. Nevertheless, the projected range reduction in the Caucasus region and northern Iran highlights their importance as long-term refugia, possibly related to higher humidity, stronger environmental and climatic heterogeneity and strong vertical zonation of the forest vegetation.

(PBX) Website: <https://www.ogm.gov.tr/lang/en/Pages/Contact.aspx>

Funding: TD acknowledges funding from the Swedish Research Council (VR grant no. 2015-03986).

Competing interests: The authors have declared that no competing interests exist.

Introduction

Climate is changing more rapidly than ever: By 2020, global surface temperature has increased by 1°C relative to the mean of the years 1951–1980 [1]. Global warming is likely to reach 1.5°C between 2030 and 2052 if it will be continuing to increase at the current rate [2]. Ongoing climate warming is already causing shifts in species phenology, physiological and behavioural traits, geographical ranges, productivity, and disruption of species interactions [3–5]. Among terrestrial biomes, forests are most affected by ongoing global warming, as it not only impacts the survival rate of tree species, but also forces plants to cope with more frequently occurring extreme events such as severe droughts, floods, wildfires, etc. [6]. Since trees are the dominant species of forest ecosystems, any influence on them would cause cascading effects on the environment in terms of resource availability, local climate stability and ecosystem services [7]. Any impacts on tree species force dependent organisms to alter their life cycles and even cause their extinction in some cases [8]. Thus, understanding the fate of tree species in response to climate change is of crucial importance for conservation and management practices [4,9].

Broadleaf deciduous forests of Asia Minor occur adjacent to two major biodiversity hotspots, the Mediterranean Basin and the Caucasus [10]. The Euxine-Colchic broadleaf forests of Turkey and Georgia, and the Hyrcanian forests of northern Iran are among the most diverse temperate forest ecosystems in western Eurasia [11]. High landscape diversity in northern Turkey, Transcaucasia and northern Iran is buffering the effects of climate change and has created refugia for plant species during past glacial periods [12,13]. However, relatively little is known about how future climates will affect the distribution of broadleaf forests in these regions.

Beech (genus *Fagus*) is widely distributed across Eurasia, where it occurs in environments with sufficient rainfall and mild temperatures [14–17]. One of the most common broadleaf species of western Eurasia is the Oriental beech (*Fagus orientalis* Lipsky), which plays an important role in forming pure or mixed beech-conifer forests. This species occupies a narrow ecological niche being sensitive to late spring frosts and summer drought [18]. Consequently, it has been identified as especially vulnerable to climate change effects [19–21]. Since *F. orientalis* acts as a keystone species in its habitat and serves as an important resource to ecosystem services such as plywood, particleboard, furniture, flooring veneer, mining poles, railway tiles, paper, and firewood [22,23], it is of paramount importance to understand the fate of this species under climate change.

The common approach to investigate the impacts of climate change on plant distributions is using species distribution models (SDMs) [24,25]. These models help to identify regions in an area with changing environmental variables that have similar conditions to localities where the species has been recorded. By using occurrence (presence/absence) and abiotic environmental data, SDMs are frequently used as a tool for estimating the extent of a species' range in the future or in the past [25,26]. Although a large number of authors have applied SDM to European woody species extensively in order to understand past and future distributions (e.g. [24–30]), there is a paucity of studies focused on Minor Asian tree taxa (e.g. [31,32]). Likewise, a great number of palaeobotanical studies investigated the late Quaternary history of *Fagus sylvatica* L. in Europe (e.g. [33–36]), and these studies were integrated with phylogeographic investigations (e.g. [37]).

In this study, we investigated the potential distribution of the Oriental beech in the past and in the future. To that end, we applied five SDM algorithms provided with the R-package 'biomod2' to model potential distributions of this species under the present (1960–1990), past [Last Glacial Maximum (LGM), 21 ka, and mid-Holocene (MH), 6 ka], and future (Representative Concentration Pathway (RCP) 2.6, 4.5 and 8.5 for 2050 and 2070) climatic conditions obtained from MIROC-ESM and CCSM4 global climate models. Specifically, we pursue the following objectives: (i) to model the present distribution of *F. orientalis*, (ii) to reconstruct

potential late Quaternary refugia of *F. orientalis*, (iii) to investigate the late Quaternary history of *Fagus* based on published palynological data, and finally, (iv) to project the future distribution of *F. orientalis* under different climate change scenarios.

Materials and methods

Study region and occurrence data

The study region (22°–54° E 35°–47° N) is defined by the observed distribution range of *F. orientalis* with some extensions for possible future or past range expansions. Occurrence data were obtained from forest management plans of the General Directorate of Forestry of Turkey (GDF) for the distribution of the species in Turkey and the European Forest Genetic Resources Program (*F. orientalis*–EUFORGEN [38]) for the remaining areas. We merged these two layers of data in ArcGIS (version 10.3.1) and created a single, presence-only dataset (Fig 1) to be used in the models. All occurrence points, obtained from EUFORGEN and GDF, were transformed into 2.5' spatial resolution using ArcGIS, generating 10,493 presence points for 457,681 raster cells across the study area.

Environmental parameters

Since the climate is the main abiotic factor shaping species distribution [24], we used nine of 19 bioclimatic variables obtained from WorldClim version 1.4 [39] as the main environmental

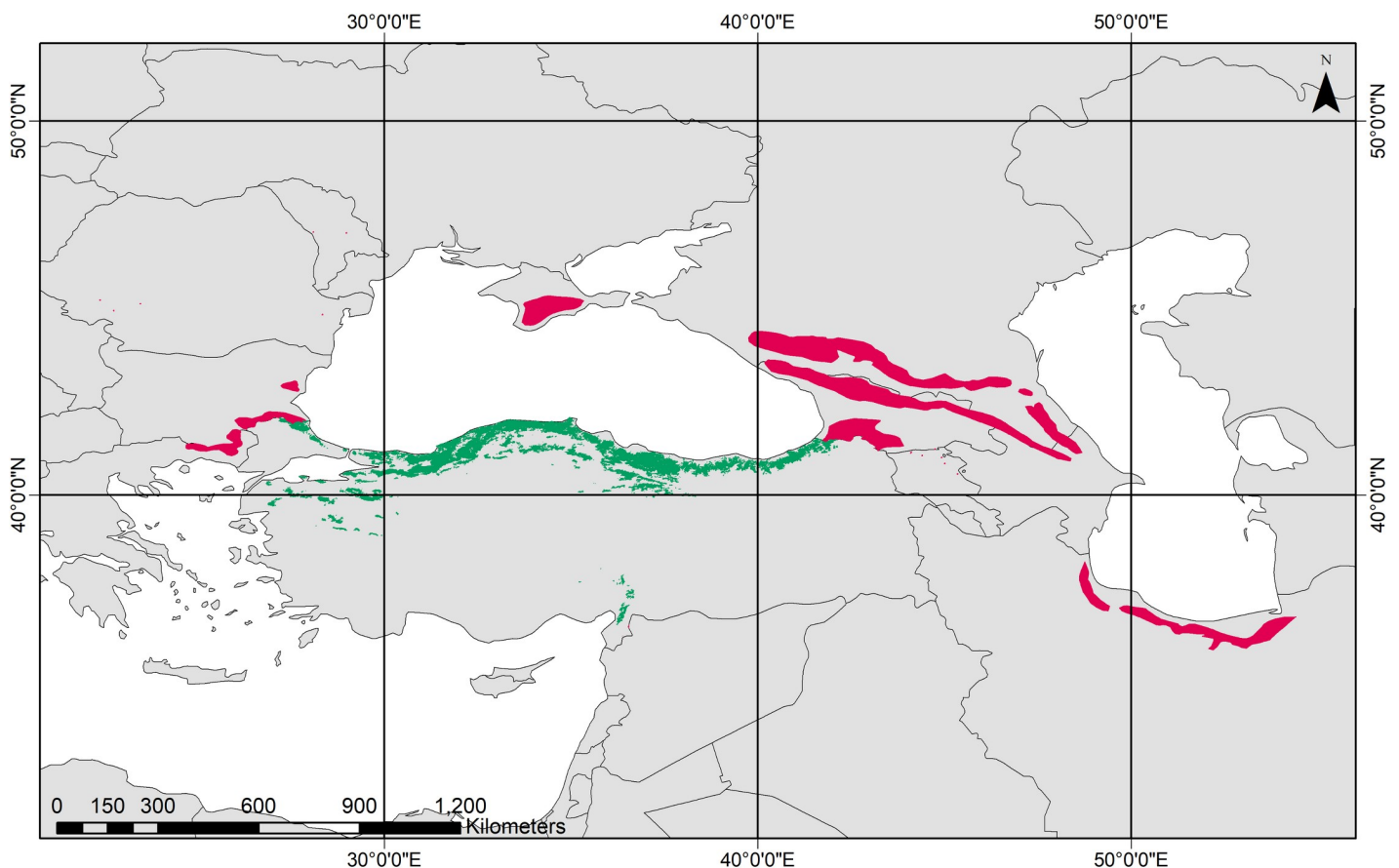


Fig 1. Modern range of *F. orientalis* based on occurrence data from EUFORGEN (red) and General Directorate of Forestry of Turkey (green).

<https://doi.org/10.1371/journal.pone.0242280.g001>

parameters (see [S1 Table](#)). The WorldClim dataset offers global climate model (GCM) simulations for the past (LGM and MH) and future (2050 and 2070) climatic conditions. We used MIROC-ESM and CCSM4 global climate simulations since they were the only two GCMs that provided data for all focal periods [40,41]. In addition, for the future simulations, climate scenarios based on IPCC reports were used [2]. According to these scenarios, in 2100, the expected CO₂ levels will be 450 ppm, 650 ppm, and 1350 ppm in optimistic, moderate, and pessimistic scenarios, respectively. In addition, the expected increase in mean annual temperature will be 0.2–1.8°C, 1.0–2.6°C, and 2.6–4.8°C, in optimistic, moderate, and pessimistic scenarios, respectively [2]. To avoid issues arising from predictor collinearity, we retained only those bioclimatic variables with low correlation ($|r| < 0.85$) (Table 1, [42,43]). As a result, we used a subset consisting of nine bioclimatic variables (Table 2). In addition, the particular ecology of beech forests was taken into account when reducing the collinearity within the environmental parameters. According to Salamon-Albert et al. [44], temperature variables (annual mean, warmest, and coldest seasonal values) determine the distribution of beech forests. For Oriental beech forests at the latitudes covering our study region both temperature and precipitation factors play important roles. In addition, accounting for both temperature and precipitation in the model structure is important to consider water and moisture availability [45].

Model structure and analysis

SDMs can describe or predict the probability of the presence or absence of a species across environmental gradients or in a specified geographical area [46]. We used the R-package ‘biomod2’ version 3.3–7.1 [47] to create potential-distribution maps of *F. orientalis*. To evaluate model performance, we implemented five different algorithms commonly used for SDMs provided with ‘biomod2’: Generalized linear model (GLM), general additive model (GAM), random forest (RF), BIOCLIM, and maximum entropy (MaxEnt). MaxEnt uses presence-only data. In contrast, GLM, GAM, and RF require both presence and absence data, and BIOCLIM uses pseudoabsence data [47], thus, we introduced 20,796 random background points to increase precision, as these add uniformity to the model while still subjected to climatic constraints [45]. Default settings were used for data formatting; 70% of the input data was used as a training sample. The related code is provided in the supplementary ([S1 File](#)).

Past and future climates were projected through the trained model, which is based on present conditions with observed distribution data. To evaluate and compare the model performances we used the Receiver Operating Characteristic Curve (Area Under the Curve, AUC) which takes values between 0 and 1 (AUC > 0.5 indicating that the model performed better than random), higher AUC value meaning better model performance [48]. Model outputs are given as the species’ presence probability in all algorithms.

To display and evaluate possible distributions we used both lowest predicted value [49] and sensitivity–specificity equality [50] methods to set a threshold for the minimum predicted value of observed occurrences, which was calculated as 0.585. We aimed at zero omission by setting this threshold and tried to balance sensitivity and specificity for increased accuracy.

Fossil pollen data

To compare and test model performances for past projections we compiled published palynological records of *Fagus* comprising LGM and MH for the range of *F. orientalis*. Although *Fagus* pollen had low values in several pollen diagrams pointing to extra-local origin of the mother plant (e.g. [51]), we accepted such records as evidence for presence of oriental beech in the region during target periods (LGM, MH).

Table 1. Correlation matrix between 19 bioclimatic variables.

VARIABLES	BIO1	BIO10	BIO11	BIO12	BIO13	BIO14	BIO15	BIO16	BIO17	BIO18	BIO19	BIO2	BIO3	BIO4	BIO5	BIO6	BIO7	BIO8	BIO9
BIO1	1,00																		
BIO10	0,97	1,00																	
BIO11	0,96	0,87	1,00																
BIO12	-0,45	-0,56	-0,29	1,00															
BIO13	-0,59	-0,65	-0,46	0,90	1,00														
BIO14	-0,21	-0,32	-0,06	0,86	0,60	1,00													
BIO15	-0,17	-0,04	-0,31	-0,46	-0,10	-0,77	1,00												
BIO16	-0,59	-0,66	-0,46	0,91	0,99	0,60	-0,10	1,00											
BIO17	-0,21	-0,32	-0,05	0,87	0,60	0,99	-0,78	0,61	1,00										
BIO18	-0,68	-0,68	-0,61	0,82	0,87	0,61	-0,17	0,87	0,61	1,00									
BIO19	0,26	0,08	0,44	0,53	0,30	0,64	-0,61	0,30	0,64	-0,02	1,00								
BIO2	-0,09	0,00	-0,22	-0,32	-0,25	-0,34	0,50	-0,24	-0,36	-0,23	-0,28	1,00							
BIO3	-0,19	-0,29	-0,07	0,23	0,19	0,15	0,05	0,20	0,14	0,01	0,31	0,62	1,00						
BIO4	0,19	0,42	-0,09	-0,61	-0,47	-0,55	0,50	-0,47	-0,56	-0,25	-0,64	0,41	-0,44	1,00					
BIO5	0,93	0,98	0,80	-0,63	-0,71	-0,40	0,06	-0,71	-0,41	-0,74	0,02	0,20	-0,18	0,49	1,00				
BIO6	0,92	0,81	0,99	-0,20	-0,38	0,01	-0,38	-0,38	0,02	-0,54	0,49	-0,37	-0,15	-0,18	0,72	1,00			
BIO7	0,03	0,24	-0,23	-0,58	-0,45	-0,56	0,59	-0,45	-0,57	-0,28	-0,62	0,75	-0,05	0,90	0,39	-0,36	1,00		
BIO8	-0,15	-0,08	-0,23	0,25	0,33	0,11	0,11	0,32	0,12	0,51	-0,36	-0,08	-0,25	0,25	-0,11	-0,21	0,13	1,00	
BIO9	0,81	0,75	0,81	-0,56	-0,67	-0,37	-0,01	-0,66	-0,37	-0,87	0,31	0,14	0,13	0,03	0,78	0,75	0,04	-0,51	1,00

The bioclimatic variables selected for the present study are highlighted in red.

<https://doi.org/10.1371/journal.pone.0242280.t001>

Phylogeographic and taxonomic framework and inferred glacial refugia

In general, populations of *F. orientalis* are markedly more differentiated than *F. sylvatica* L. with F_{ST} (coefficient of differentiation among populations) being 0.157 in the former and 0.032 in the latter. In addition, much higher levels of allelic richness in this species indicating that Pleistocene bottlenecks did not deplete the gene pool to the extent they did in the European *F. sylvatica* [52]. Geographical subgroups of *F. orientalis* are morphologically and genetically highly distinct [52–56]. Populations ranging from eastern Bulgaria to northern Turkey and the Amanos Mountains form one cluster. Two additional highly distinct clusters involve the Caucasian populations on the one hand and the populations south of the Caspian Sea on the other hand. In contrast, the European *F. sylvatica* forms a single cluster [52]. In a recent study, Gömöry et al. [56] tested speciation scenarios in subgroups of *F. orientalis* under an approximate Bayesian framework. The number of generations was used to estimate divergence times between genetically distinct regional populations. Divergence times suggest that European populations of *F. sylvatica* diverged from Asian Minor populations (*F. orientalis*) at c. 1.222–0.7 Ma. The Crimean beech is a hybrid between Caucasian *F. orientalis* and *F. sylvatica*. It might have originated at around the Eemian interglacial (130–114 ka). Differentiation among the eastern populations happened much earlier: Caspian populations become isolated from Caucasian ones at 2.2–1.6 Ma, and from Turkish ones at 1.9–1.8 Ma. Finally, genetic isolation between populations of *F. sylvatica* from the Balkans and Central Europe and Apennine occurred much later, at 100 ka and 70 ka. This has important implications for inferring Pleistocene refugia for beech in western Eurasia. Essentially, when considering LGM and MH, *in situ* refugia must have existed for all geographical subgroups of *F. orientalis* because these regional groups had been isolated long before these events.

Table 2. Bioclimatic variables (precomputed in WorldClim dataset) used as environmental input in the models.

Abbreviations	Bioclimatic variables	Unit
BIO1	Annual Mean Temperature	°C
BIO2	Mean Diurnal Range	°C
BIO3	Isothermality	-
BIO4	Temperature Seasonality	°C
BIO8	Mean Temperature of Wettest Quarter	°C
BIO9	Mean Temperature of Driest Quarter	°C
BIO12	Annual Precipitation	mm
BIO15	Precipitation Seasonality	mm
BIO19	Precipitation of Coldest Quarter	mm

<https://doi.org/10.1371/journal.pone.0242280.t002>

Results

Model evaluation and environmental parameters relevant for *Fagus orientalis* growth in Asia Minor

The results are indicating that models were good in distinguishing presence data from the background based on their AUC values varying from 0.79 to 0.99 (all > 0.7, Table 3, [57]). According to this, the best-fit algorithm was RF and the worst-fit was BIOCLIM. In the following, we will focus on the RF algorithm provided with 'biomod2', which fitted best for *F. orientalis*. Successful model results from the present climate could be used to identify and evaluate optimal environmental conditions for *F. orientalis* growth. The projections for the past, MH and LGM, and for the future, 2050 and 2070, gave different distributions with different climate change scenarios and global climate models (S1–S10 Figs).

Past projections

Projections for the LGM at 21 ka and the MH at 6 ka from two different global climate models gave consistent results. Past projection outputs of RF are shown with the pollen records collected from published palynological studies of *Fagus* during LGM and MH (Fig 2). The model outputs show that the possible distribution of *Fagus* was mainly from the mid-Black Sea region to Caucasia and northern Iran to southern Turkmenistan during the LGM (Fig 2A). Additionally, RF predicted a refuge area in the Amanos region during the LGM. For the MH, the populations ranging from the mid-Black Sea region to Caucasia remained in these regions, whereas, the Iranian/Turkmen region almost lost its population, except some patches. During the MH, species distribution shifted towards the west, especially towards Europe and western Anatolia (Fig 2B). Outputs arising from other algorithms are shown in S1–S10 Figs.

Late Quaternary palynological records of *Fagus* in Asia Minor

A general feature of the 30 pollen profiles containing *Fagus* is the sparse occurrence or absence of this genus during the LGM and its more or less continuous presence since about 10 ka (Fig 2 and Table 4). LGM values are usually low indicating long distance dispersal (LDD). One

Table 3. AUC_{test} values of all the algorithms, bioclim, maximum entropy (MaxEnt), generalized additive model (GAM), generalized linear model (GLM), and random forest (RF) performed with present climate conditions (1960–1990).

Algorithm	BIOCLIM	MaxEnt	GAM	GLM	RF
AUC _{test}	0.79	0.94	0.96	0.93	0.99

<https://doi.org/10.1371/journal.pone.0242280.t003>

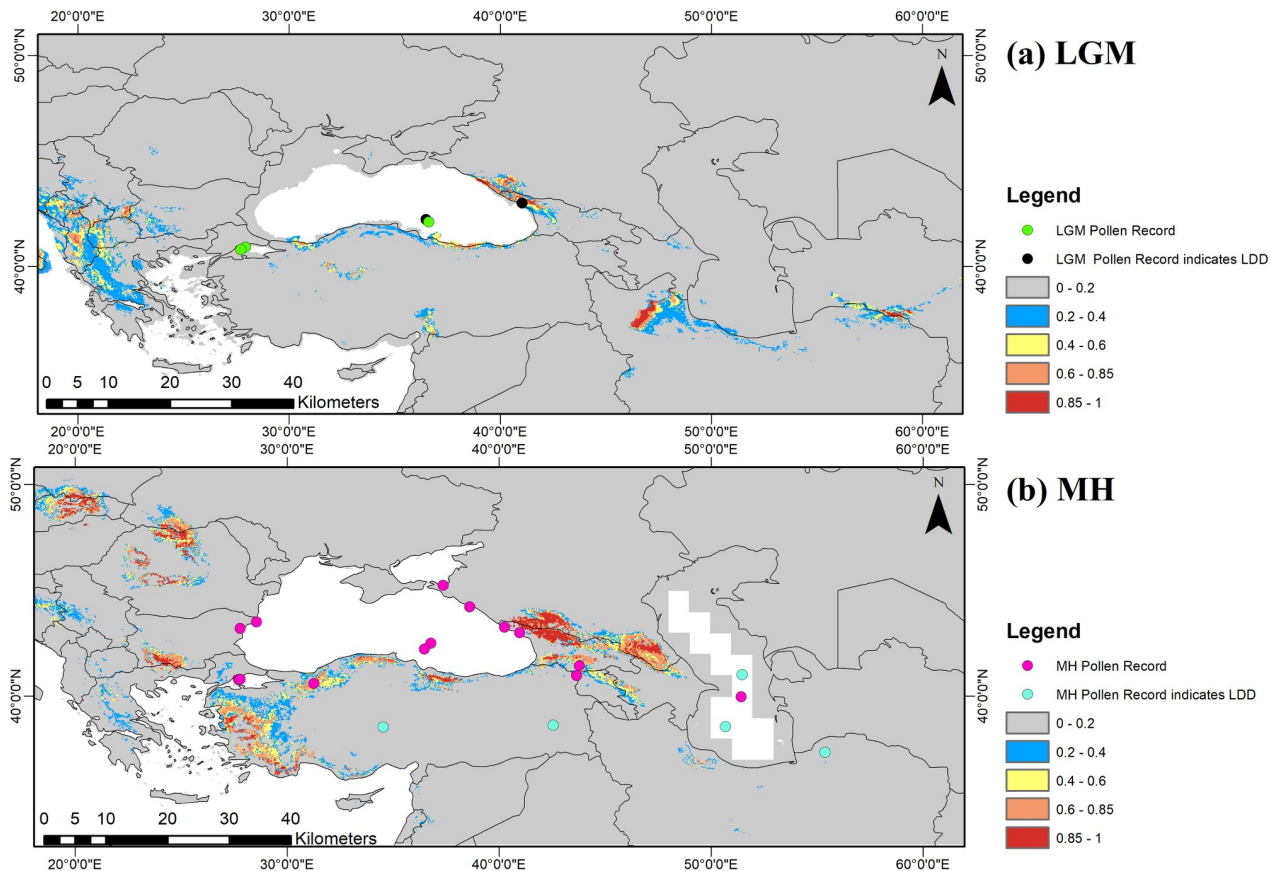


Fig 2. Past range projections with random forest algorithm; here only MIROC-ESM is shown (for CCSM4 see S8 Fig). Occurrence probability of the species is increasing from grey to red (absence to presence) for a) LGM and b) MH. Dots are indicating pollen records (Table 4).

<https://doi.org/10.1371/journal.pone.0242280.g002>

exception is the profile from the Sea of Marmara (core MD01-2430) that records beech with moderate abundance during the LGM. No suitable sediments recording the plant cover during the LGM are known from the southern Caspian area. This might be due to the marked drop in sea level (-50 m) of the Caspian Sea during this period [82]. In contrast, MH distribution of *F. orientalis* was continuous and abundant throughout its present range from eastern Bulgaria, the Sea of Marmara, northern Turkey, Crimea, the western Caucasus, and the southern Caspian Sea region. Percentages commonly are way above the proposed threshold values indicating local presence of *Fagus* reported in Lisitsyna et al. [51]. Moreover, we did not find convincing evidence for the presence of beech during MH outside its present distribution range. Two pollen profiles from Cappadocia and Lake Van have sporadic occurrences of *Fagus* pollen but these are very few pollen grains and most likely indicate LDD. This is also suggested by the overall composition of these pollen floras (open oak woodland in the Acıgöl area of Cappadocia [69], forest steppe in the Lake Van area [70]).

Future projections

The combined results from both global climate models with different scenarios show that in the future, the main geographical shift of *F. orientalis* will be towards the northeast of its present distribution. According to the RF model, a severe range contraction of the species is expected in relation to the present distribution provided by the projected model and the

compiled occurrence data (Table 5 and Fig 1). In addition, a refuge area was projected southwest of the Caspian Sea including the southwestern Caspian coastal area and coastal mountains (Fig 3, for additional algorithms see S1–S10 Figs). The proportion of species presence in the RF MIROC-ESM projections from different scenarios is shown in Table 5. According to the table, the proportion of presence cells is 1.49% in the optimistic, 0.95% in the moderate, and 0.42% in the pessimistic climate scenario. Details of the spatial changes are shown in Fig 3.

Table 4. Palaeobotanical records for the LGM and MH [58–81].

Country	Locality/site	LGM	MH	Pollen record	<i>Fagus</i> presence
Bulgaria	Black Sea Core GGC-18	No data	Present	12 ka	Cont. since 11 ka
Bulgaria	Varna Lake/Core 3	No data	Present	8 ka	Continuous
Bulgaria	W Black Sea	No data	Present	12 ka	Increase at c. 7 ka
Greece	Lesbos/Megali Limni 01	Absent	Absent	62–22 ka	Present at c. 32 ka, LDD
NW Turkey	Marmaris/MAR94-5	Present	Hiatus	30 ka	Continuous
NW Turkey	Marmaris/Core MD01-2430	Present	Present	23 ka	Continuous
NW Turkey	Marmaris/MAR98-12	No data	Present	c. 17 ka	Peak at HM
NW Turkey	Marmaris/MAR98-13	No data	Present	c. 18 ka	Peak at HM
NW Turkey	Black Sea/Core B-7	No data	Present	c. 12 ka	Peak at HM
NC Turkey	Yeniçağa, Bolu	No data	Present	c. 12 ka	Increase since c. 7 ka
NC Turkey	Abant Gölü, Bolu	No data	Present	c. 10 ka	Increase since c. 10 ka
NC Turkey	Black Sea/Core 22-GC3	Present, LDD	Present	18 ka	Cont., rapid increase at 8.5 ka
NC Turkey	Black Sea/Core 22-GC3/8	No data	No data	134–119 ka	Cont., rapid increase at 126 ka
NC Turkey	Black Sea/Core 25-GC1	Present	No data	63–19 ka	No specific information
C Turkey	Cappadocica/Eski Acıgöl I, II	No data	Present, LDD	15.6 ka	Sporadic, LDD
SE Turkey	Söğütlü, Van	No data	Absent	7 ka	Sporadic since c. 5 ka, LDD
SE Turkey	Lake Van/Core 90–04	No data	Present, LDD	12 ka	Sporadic since 10 ka, LDD
Georgia	Sukhumi/ Core no 723	No data	Present	c. 10 ka	Continuous
Georgia	Sukhumi/Dziguta Core 1	Present, LDD	No data	48–9 ka	Increase at c. 13 ka
Georgia	NE Black Sea/Core Ak-2575	No data	Present	10 ka	Continuous
Georgia	E Black Sea/Gagra, Core no 471	No data	Present	10 ka	Continuous
Georgia	Various sites	Present	No data	18±2 ka	No information
Iran	Lake Urmia	Absent	Absent	200 ka	Absent
Iran	Caspian Sea/Core CP14	No data	Present	5 ka	Continuous
Iran	Caspian Sea/Core GS18	No data	Present, LDD	12–2 ka	Cont. low, LDD
Iran	Caspian Sea/Core GS05	No data	Present, LDD	15 ka	Sporadic since c. 9 ka, LDD
NE Iran	Kongor Lake	No data	Present, LDD	6 ka	Discont. low, LDD

<https://doi.org/10.1371/journal.pone.0242280.t004>

Table 5. Spatial cell numbers of contraction, overlap, and expansion shown in Fig 3 are quantified in this table.

Period	Future Scenario	Expected Contraction	Expected Contraction in model	Overlap	Expected Expansion	Overlap with observed occurrence data (%)
Present	–	115	–	10,372	9,444	98.85
2070	RCP 2.6	7,944	7919	3,954	1,558	37.68
	RCP 4.5	9,009	8226	2,582	927	24.61
	RCP 8.5	9,816	8914	1,087	446	10.36

Overlap of the species occurrence between the observed data and model outputs are given as percentages. In future projections, from optimistic to pessimistic scenario, contractions are increasing, overlap and expansion are decreasing.

<https://doi.org/10.1371/journal.pone.0242280.t005>

Discussion

Model evaluation for different SDM algorithms

Modelling the spatial distribution of *F. orientalis* provided details of the species responses to different climate change scenarios and identified possible past refugia by means of projected past distributions and palynological data. A key assumption of SDM with bioclimatic variables is that the ranges of the modelled species are in equilibrium with climate [25, 29, 83]. In general, the modelled present distributions fitted reasonably well with the observed distribution data, which allowed us to use the trained model for past and future simulations. As mentioned before, all models ran successfully according to their AUC values (Table 3), and the combination of regression and classification approaches, as well as the in-algorithm verification process provided more accurate outcomes in RF and made this algorithm the most successful one [84]. On the other hand, according to the AUC values (Table 3) the least successful algorithm was BIOCLIM. Due to the advanced characteristics and calculations of other algorithms, it was expected that they would give a better fit than BIOCLIM. One problematic algorithm was GAM (S5 and S6 Figs) with a very wide distribution of Oriental beech projected for LGM and MH. Although GAM has the second-best AUC value, we interpreted this as an overfitted distribution. It is known that this algorithm is highly sensitive to large sample size since the fitted functions are not constrained to any functional form when sample size increases [85]. Further, it is noteworthy that while there are substantial differences between modelling performances from different algorithms, the outcomes are consistent, which is a hint for repeatability [86].

The present distribution of Oriental beech

The present distribution of *Fagus orientalis* in the RF algorithm/MIROC-ESM was largely congruent with the observed presence records (Figs 1 and 3A), which is also illustrated by its high AUC value. A range expansion in the European region (Fig 3A) most probably reflects similar present growing conditions of *F. orientalis* and its sister species *F. sylvatica*. Hence, it is not surprising that models recognize habitats of *F. sylvatica* as suitable for *F. orientalis* [8, 17]. Although there is a close match between observed and modelled distribution, it is interesting to note that the model predicted range expansion to the south of the Pontic Mountains (Kuzey Anadolu Dağları). Under present conditions, this is unlikely as the rain shadow south of the main ridge of the Pontic Mountains creates a sharp change from fully humid Cf climates (see [16, 87]) to Mediterranean Cs and continental, arid BS climates. Whereas, *Fagus* is replaced by Pinaceae at higher elevations, it is replaced by *Quercus* species (e.g. *Quercus macranthera* Fisch. et Mey.) both at higher elevations and in drier areas beyond the main ridge [88].

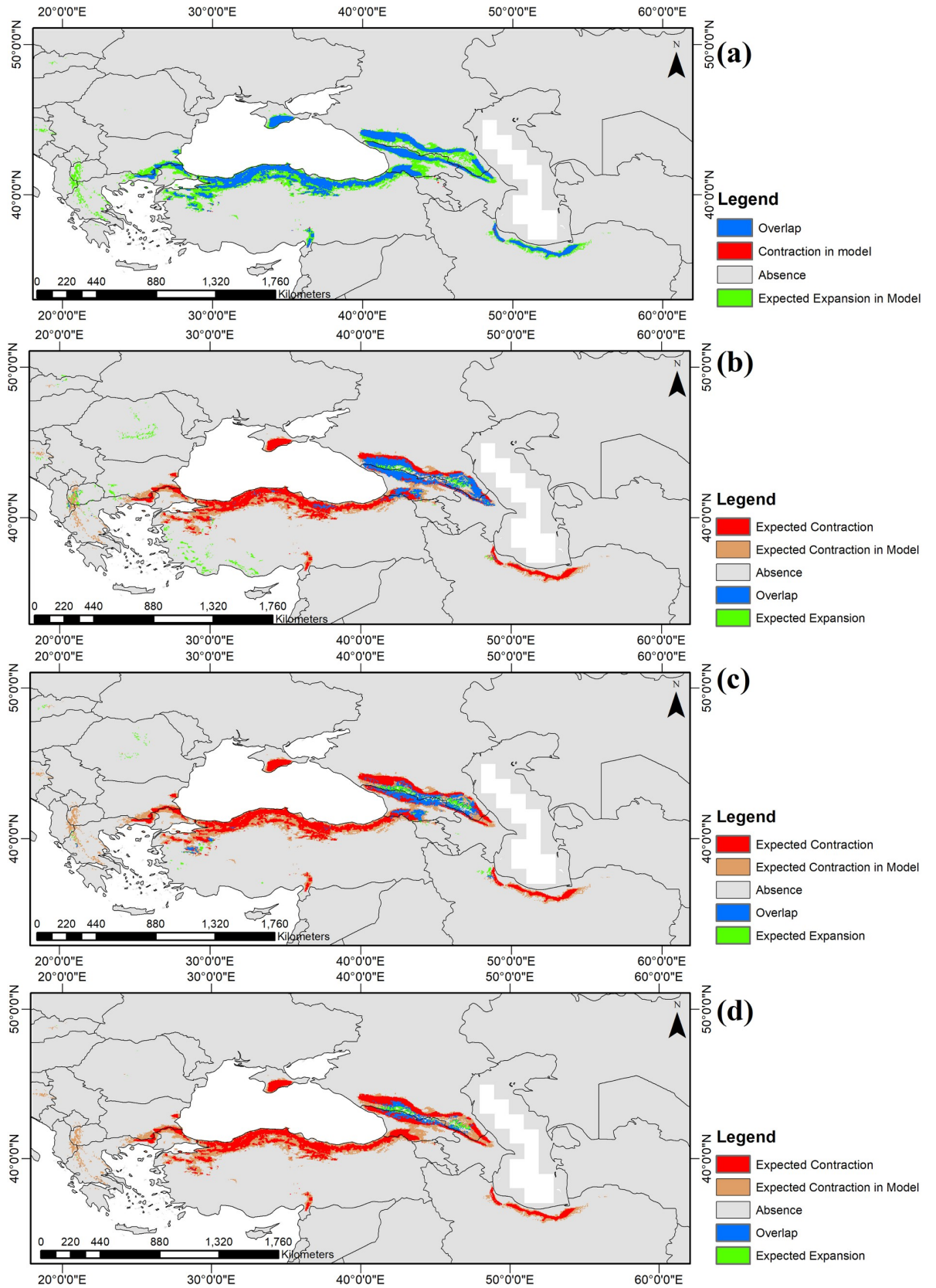


Fig 3. Distribution maps of present and future projections of *F. orientalis* are shown from the random forests outputs of a) present, b) optimistic future scenario RCP 2.6, c) moderate future scenario RCP 4.5, and d) pessimistic future scenario RCP 8.5. Red areas show the contraction of species occurrence based on observed data and future projections, brown areas show the contraction of species occurrence based on present and future projections, blue areas represent overlap of species occurrence based on observed data and present projection, green areas show the expansion of species occurrence based on observed data and projections. We quantified the cell numbers for each category in Table 5. Spatial resolution: 2.5'.

<https://doi.org/10.1371/journal.pone.0242280.g003>

The situation is similar in the Iranian Alborz Mountains, where *Quercus macranthera* replaces *Fagus* at higher elevations [89]. The Amanos Mountains are distinctive, because Oriental beech is confined to higher elevations under a distinct microclimate, thus, it is remarkable that the model could identify this relict population here [90].

Past reconstructions and palynological data comparison

Probability estimates for occurrences of Oriental beech during the LGM by 'biomod2' (Fig 2A) are to some extent congruent with known pollen records. Unambiguous occurrences of beech pollen from LGM deposits are known from the Sea of Marmara, off the central northern Turkish Black Sea coast, and from Sukhumi. These occurrences coincide with highly probable model estimates (red in Fig 2A). While estimates on presence in Transcaucasia and southwest of the Caspian Sea are sensible although not supported by palynological data, a refuge area in Turkmenistan at 60°E east of the Caspian Sea is highly unrealistic in view of the present arid climate in this region. During the LGM, a cold continental climate would not have provided suitable conditions for the growth of beech. 'biomod2' reconstructed a further refugium in the Alborz Mountains south of 35°N. Although no pollen record is available for this region, the Amanos Mountains with a high relief, deep valleys, and slopes facing the sea likely provided a refuge for beech populations during the LGM.

The core region of *F. orientalis* estimated for the MH (Fig 2B) includes the Turkish Black Sea Coast and the Caucasus. This is also suggested by unambiguous pollen records known from this area (Fig 2B and Table 4). In contrast, 'biomod2' with RF predicted a rather limited distribution south of the Caspian Sea, from where abundant pollen records of beech are known as well. Palynological data and paleoclimate modelling [91, 92] suggest that temperate regions during the MH might have been warmer than today during summer and colder during winter because of astronomical forcing. Today, fully humid, warm temperate *Cf* climates are much less common along the southern Caspian Sea coast than south of the Black Sea and along the northern and southern foothills of the Caucasus ([16]; http://koeppen-geiger.vu-wien.ac.at/kmz/Global_1986-2010_KG_5m.kmz.zip provided by Veterinary University of Vienna, <http://koeppen-geiger.vu-wien.ac.at/present.htm>). In northern Iran, a stronger Mediterranean influence is expressed by lower summer precipitation and higher summer temperatures (http://koeppen-geiger.vu-wien.ac.at/kmz/Global_1986-2010_KG_5m.kmz.zip). Hence, warmer summers during the Mid Holocene would have increased this Mediterranean influence and resulted in a much-reduced distribution of Oriental beech in the models. As today, these unfavourable conditions might have been compensated by high air moisture and a sky covered with fog for most of the year and particularly during the growing season [89]. However, the predicted presence of beech in the western corner of the Caspian coast makes sense, as this area—constrained by wind directions and high mountains to the south and a large water body to the north, very likely could have supported growth of beech during the MH (Fig 2B).

Future projections

Future projections show that *F. orientalis* will face a dramatic range contraction in the future (Figs 3B–3D and S1–S10). The projections suggest that the species will mainly thrive in the

Caucasus region. Since it is assumed that future climatic conditions will cause an increase in temperature and drought, the mountainous regions of Caucasia will be preferred by Oriental beech for possibly more suitable temperature and moisture conditions. The RF algorithm suggests a slight expansion south of the Caspian Sea, along the southwestern Caspian coast. This supports the idea of potential refugia for *F. orientalis* in the future in this region and emphasizes the importance of this region as a long-term refugium for temperate tree species. Both regions are characterized by high mountain ranges. The Alborz Mountains, located just south of the Caspian Sea, providing a barrier for humid air masses thereby creating warm and humid conditions from sea level to high elevations. This leads to a large number of suitable habitats under a changing climate as plants can move vertically. A similar situation is met in the western parts of Caucasia where humid air masses from the Black Sea create markedly humid conditions along the coast and on the slopes of the greater and lesser Caucasus (e.g [93]). Towards the east, climatic conditions become drier, but the great vertical gradient remains, thus providing a dynamic environment for tree species to respond to changing environments by vertical movements. A recent study by Martin-Benito et al. [21] supports the notion that due to little drought response and positive effects of spring-summer warmth, mid- to high-elevation sites in the Caucasus might be potential major climatic refugia for *Fagus orientalis* in the future.

Comparison with SDMs of European beech (*Fagus sylvatica*)

Process-based and statistical modelling approaches have been widely used for modelling past and future distribution of a close relative of *F. orientalis*, *Fagus sylvatica*. For instance, Gisecke et al. [27] used the process-based bioclimatic model to understand the distribution of *F. sylvatica* during the MH. In agreement with our findings, they also compared their model results with pollen records and found some mismatches, in particular in the northern and western parts of the distribution. They emphasized the need for testing models against palynological data to increase their predictive value. Likewise, a recent study modelling the modern and past distribution of deciduous oaks (*Quercus robur* L.) also showed a mismatch between the modelled LGM distribution and the one inferred from pollen data [32]. This study suggested that the more restricted distribution data from the pollen record might be due to competition of deciduous oaks with pines and Mediterranean evergreen oaks. Saltré et al. [94] applied a process-based approach coupled with migration models to assess whether the present distribution of *F. sylvatica* is controlled more by climatic conditions or the migration ability during the MH in Europe. Their findings suggested that the northeast boundary of *F. sylvatica* distribution is limited by climatic conditions whereas the northwest boundary is limited by migration ability. This is very similar to the situation in *F. orientalis*, where, clearly, the (north)eastern boundary is controlled by climate whereas the western boundary is limited by migration ability. However, in contrast to *F. sylvatica*, the westward expansion of Oriental beech is limited because it is replaced towards the west by its sister species *F. sylvatica*. Kramer et al. [95] investigated *F. sylvatica* distribution under climate change with both process-based and statistical modelling approaches. They found that statistical species distribution models exhibited a better goodness-of-fit for future projections, with the southern limit of the *F. sylvatica* distribution shifted towards the north. On the other hand, future projections of Dyderski et al. [8] for twelve European forest tree species including European beech suggested that the distribution ranges in western and southern Europe will decrease. This seems plausible in view of the predicted climate change towards summer-dry Cs climates in western and southwestern Europe during 2070–2100 ([96]; Global_Shift_A1FI_1976–2100_30m.kmz).

Conclusions

In this study, we investigated the late Quaternary history of *F. orientalis* utilizing palynological data and past reconstructions and estimated the future distribution of the species in response to global climate change. We compared model outputs to the observed present distribution of *F. orientalis* and palynological records from LGM and MH. Based on these empirical data, the RF algorithm, among five algorithms in the R-package ‘biomod2’, performed best with more plausible results for both past and future distributions. As in previous studies using *F. sylvatica* and *Quercus robur* as focal species, models tend to overestimate occurrence probabilities. For LGM and MH, the results were roughly in accord with palynological data for the Sea of Marmara and the Black Sea region, while palynological data did not support potential refugia south of the Caspian Sea during LGM. However, genetically long isolated populations of Oriental beech south of the Caspian Sea strongly suggest that they survived the LGM in-situ. For future projections, with continuing climate change, *F. orientalis* populations in the western Eurasian region will be decreasing with increasing drought; the geographical range will contract leaving only two possible refugia, the southern Caspian Sea region (northern Iran) and the Caucasus.

This study shows, albeit they can be improved by including other environmental data (e.g. aspect, soil), that our models provide crucial information on the effect of climate change on *F. orientalis* in Asia Minor even when only considering the climate. In addition, these results emphasize the importance of combining evidence from modelling with real-world data, such as the rich Quaternary pollen record of *Fagus*, to understand species-specific responses to changing environments. Hence, these results should be taken into account in order to improve conservation and management plans for this important forest species in western Eurasia.

Supporting information

S1 Table. 19 bioclimatic variables obtained from WorldClim version 1.4.
(PDF)

S1 File. R code sheet for biomod2 package to perform SDM.
(PDF)

S1 Fig. Probability distributions of *F. orientalis* predicted for the present, MH, LGM, pessimistic (RCP 8.5) 2050 and 2070, moderate (RCP 4.5) 2050 and 2070, and optimistic (RCP 2.6) 2050 and 2070 with MaxEnt algorithm and MIROC-ESM GCM.
(TIF)

S2 Fig. Probability distributions of *F. orientalis* predicted for the present, MH, LGM, pessimistic (RCP 8.5) 2050 and 2070, moderate (RCP 4.5) 2050 and 2070, and optimistic (RCP 2.6) 2050 and 2070 with MaxEnt algorithm and CCSM4 GCM.
(TIF)

S3 Fig. Probability distributions of *F. orientalis* predicted for the present, MH, LGM, pessimistic (RCP 8.5) 2050 and 2070, moderate (RCP 4.5) 2050 and 2070, and optimistic (RCP 2.6) 2050 and 2070 with GLM algorithm and MIROC-ESM GCM.
(TIF)

S4 Fig. Probability distributions of *F. orientalis* predicted for the present, MH, LGM, pessimistic (RCP 8.5) 2050 and 2070, moderate (RCP 4.5) 2050 and 2070, and optimistic (RCP 2.6) 2050 and 2070 with GLM algorithm and CCSM4 GCM.
(TIF)

S5 Fig. The probability of *F. orientalis* predicted for the present, MH, LGM, pessimistic (RCP 8.5) 2050 and 2070, moderate (RCP 4.5) 2050 and 2070, and optimistic (RCP 2.6) 2050 and 2070 with GAM algorithm and MIROC GCM.

(TIF)

S6 Fig. The probability of *F. orientalis* predicted for the present, MH, LGM, pessimistic (RCP 8.5) 2050 and 2070, moderate (RCP 4.5) 2050 and 2070, and optimistic (RCP 2.6) 2050 and 2070 with GAM algorithm and CCSM4 GCM.

(TIF)

S7 Fig. Probability distributions of *F. orientalis* predicted for the present, MH, LGM, pessimistic (RCP 8.5) 2050 and 2070, moderate (RCP 4.5) 2050 and 2070, and optimistic (RCP 2.6) 2050 and 2070 with RF algorithm and MIROC-ESM GCM.

(TIF)

S8 Fig. Probability distributions of *F. orientalis* predicted for the present, MH, LGM, pessimistic (RCP 8.5) 2050 and 2070, moderate (RCP 4.5) 2050 and 2070, and optimistic (RCP 2.6) 2050 and 2070 with RF algorithm and CCSM4 GCM.

(TIF)

S9 Fig. Probability distributions of *F. orientalis* predicted for the present, MH, LGM, pessimistic (RCP 8.5) 2050 and 2070, moderate (RCP 4.5) 2050 and 2070, and optimistic (RCP 2.6) 2050 and 2070 with BIOCLIM algorithm and MIROC-ESM GCM.

(TIF)

S10 Fig. Probability distributions of *F. orientalis* predicted for the present, MH, LGM, pessimistic (RCP 8.5) 2050 and 2070, moderate (RCP 4.5) 2050 and 2070, and optimistic (RCP 2.6) 2050 and 2070 with BIOCLIM algorithm and CCSM4 GCM.

(TIF)

Acknowledgments

We are thankful to Abbas Şahin and the General Directorate of Forestry, Turkey, for providing *Fagus* distribution data in Turkey. Valuable comments of two anonymous reviewers helped improving the final manuscript.

Author Contributions

Conceptualization: Dilsad Dagtekin, Evrim A. Şahan, Nesibe Köse, H. Nüzhet Dalfes.

Data curation: Dilsad Dagtekin, Evrim A. Şahan, Thomas Denk, Nesibe Köse, H. Nüzhet Dalfes.

Formal analysis: Dilsad Dagtekin, Evrim A. Şahan, H. Nüzhet Dalfes.

Funding acquisition: Thomas Denk.

Investigation: Dilsad Dagtekin, H. Nüzhet Dalfes.

Methodology: Dilsad Dagtekin, Evrim A. Şahan, Thomas Denk, Nesibe Köse, H. Nüzhet Dalfes.

Project administration: Nesibe Köse, H. Nüzhet Dalfes.

Resources: Thomas Denk, Nesibe Köse, H. Nüzhet Dalfes.

Software: Dilsad Dagtekin, Evrim A. Şahan, H. Nüzhet Dalfes.

Supervision: Nesibe Köse, H. Nüzhet Dalfes.

Validation: Dilsad Dagtekin, Evrim A. Şahan, Thomas Denk, Nesibe Köse, H. Nüzhet Dalfes.

Visualization: Dilsad Dagtekin, Evrim A. Şahan, H. Nüzhet Dalfes.

Writing – original draft: Dilsad Dagtekin, Evrim A. Şahan, Thomas Denk, Nesibe Köse, H. Nüzhet Dalfes.

Writing – review & editing: Dilsad Dagtekin, Evrim A. Şahan, Thomas Denk, Nesibe Köse, H. Nüzhet Dalfes.

References

1. Vital Signs of the Planet. [cited 07 September 2020]. In: NASA 2020 Global Climate Change [Internet]. Available from: <https://climate.nasa.gov/vital-signs/global-temperature/>
2. IPCC, 2018: Summary for Policymakers. In: Global Warming of 1.5°C. An IPCC Special Report on the impacts of global warming of 1.5°C above pre-industrial levels and related global greenhouse gas emission pathways, in the context of strengthening the global response to the threat of climate change, sustainable development, and efforts to eradicate poverty [Masson-Delmotte V., Zhai P., Pörtner H.-O., Roberts D., Skea J., Shukla P.R., Pirani A., Moufouma-Okia W., Péan C., Pidcock R., Connors S., Matthews J.B.R., Chen Y., Zhou X., Gomis M.I., Lonnoy E., Maycock T., Tignor M., and Waterfield T. (eds.)]. World Meteorological Organization, Geneva, Switzerland, 32 pp.
3. Walther GR, Post E, Convey P, Menzel A, Parmesan C, Beebee TJ, et al. Ecological responses to recent climate change. *Nature*. 2002; 416(6879):389–395. <https://doi.org/10.1038/416389a> PMID: 11919621
4. Parmesan C. Ecological and evolutionary responses to recent climate change. *Annu. Rev. Ecol. Evol. Syst.* 2006; 37:637–669.
5. Scheffers BR, De Meester L, Bridge TC, Hoffmann AA, Pandolfi JM, Corlett RT, et al. The broad footprint of climate change from genes to biomes to people. *Science*. 2016; 354(6313): 719–730.
6. Lindner M, Maroschek M, Netherer S, Kremer A, Barbatí A, Garcia-Gonzalo J, et al. Climate change impacts, adaptive capacity, and vulnerability of European forest ecosystems. *For. Ecol. Manage.* 2010; 259(4):698–709.
7. Boisvenue C, Running SW. Impacts of climate change on natural forest productivity—Evidence since the middle of the 20th century. *Glob. Change Biol.* 2006; 12(5):862–82.
8. Dyderski MK, Paž S, Frelich LE, Jagodziński AM. How much does climate change threaten European forest tree species distributions?. *Glob. Change Biol.* 2018; 24(3):1150–63. <https://doi.org/10.1111/gcb.13925> PMID: 28991410
9. Root TL, Schneider SH. Conservation and climate change: the challenges ahead. *Cons. Biol.* 2006; 20(3): 706–8. <https://doi.org/10.1111/j.1523-1739.2006.00465.x> PMID: 16909561
10. Myers N, Mittermeier RA, Mittermeier CG, Da Fonseca GA, Kent J. Biodiversity hotspots for conservation priorities. *Nature*. 2000; 403(6772): 853. <https://doi.org/10.1038/35002501> PMID: 10706275
11. Temperate broadleaf and mixed forests. [cited March 2019]. In: World Wildlife Fund, WWF [Internet]. Available from: <https://www.worldwildlife.org/biomes/temperate-broadleaf-and-mixed-forests>
12. Médail F, Diadema K. Glacial refugia influence plant diversity patterns in the Mediterranean Basin. *J. Biogeogr.* 2009; 36(7): 1333–45.
13. Şekercioğlu ÇH, Anderson S, Akçay E, Bilgin R, Can ÖE, Semiz G, et al. Turkey's globally important biodiversity in crisis. *Biol Conserv.* 2011; 144(12): 2752–69.
14. Yaltrınk F, & Eliçin G. Trees and Shrubs in European Turkey. *İstanbul Üniversitesi Orman Fakültesi Dergisi A*. 1982; 32(2).
15. Fang J, Lechowicz MJ. Climatic limits for the present distribution of beech (*Fagus L.*) species in the world. *J. Biogeogr.* 2006; 33(10): 1804–19.
16. Kottek M, Grieser J, Beck C, Rudolf B, Rubel F. World map of the Köppen-Geiger climate classification updated. *Meteorol. Z.* 2006; 15(3): 259–63.
17. Caudullo G, Welk E, San-Miguel-Ayanz J. Chorological maps for the main European woody species. Data in brief. 2017; 12: 662–666. <https://doi.org/10.1016/j.dib.2017.05.007> PMID: 28560272
18. Peters R. Beech Forests: Woody Species Composition, Populations and Spatial Aspects. In: *Beech Forests*. Dordrecht: Springer;1997. p. 89–130.

19. Köse N, Güner HT. The effect of temperature and precipitation on the intra-annual radial growth of *Fagus orientalis* Lipsky in Artvin, Turkey. *Turk. J. Agric. For.* 2012; 36(4): 501–9.
20. Haghshenas M, Mohadjer MR, Attarod P, Pourtahmasi K, Feldhaus J, Sadeghi SM. Climate effect on tree-ring widths of *Fagus orientalis* in the Caspian forests, northern Iran. *Forest Sci. Technol.* 2016; 12(4): 176–82.
21. Martin-Benito D, Pederson N, Köse N, Doğan M, Bugmann H, Mosulishvili M, et al. Pervasive effects of drought on tree growth across a wide climatic gradient in the temperate forests of the Caucasus. *Glob. Ecol. Biogeogr.* 2018; 27(11): 1314–25.
22. Kandemir G, Kaya Z. EUFORGEN [European Forest Genetic Resources Programme] technical guidelines for genetic conservation and use for oriental beech (*Fagus orientalis*). EUFORGEN Technical Guidelines for Genetic Conservation and Use. 2009.
23. Bozkurt AY, Erdin N. Ağaç Teknolojisi Ders Kitabı, İstanbul Üniversitesi Orman Fak. Orman End. Müh. Böl., 372s. İstanbul. 1997.
24. Pearson RG, Dawson TP. Predicting the impacts of climate change on the distribution of species: are bioclimate envelope models useful? *Glob. Ecol. Biogeogr.* 2003; 12(5): 361–71.
25. Pearson RG. Species' distribution modeling for conservation educators and practitioners. *Synthesis. Am. Mus. Nat. Hist.* 2007; 50: 54–89.
26. Elith J, Leathwick JR. Species distribution models: ecological explanation and prediction across space and time. *Annu. Rev. Ecol. Evol. Syst.* 2009; 40: 677–97.
27. Giesecke T, Hickler T, Kunkel T, Sykes MT, Bradshaw RH. Towards an understanding of the Holocene distribution of *Fagus sylvatica* L. *J. Biogeogr.* 2007; 34(1): 118–31.
28. Benito Garzón M, Sánchez de Dios R, Sáinz Ollero H. Predictive modelling of tree species distributions on the Iberian Peninsula during the Last Glacial Maximum and Mid-Holocene. *Ecography.* 2007; 30(1): 120–34.
29. Svenning JC, Normand S, Kageyama M. Glacial refugia of temperate trees in Europe: insights from species distribution modelling. *J. Ecol.* 2008; 96(6): 1117–27.
30. Maiorano L, Cheddadi R, Zimmermann NE, Pellissier L, Petitpierre B, Pottier J, et al. Building the niche through time: using 13,000 years of data to predict the effects of climate change on three tree species in Europe. *Glob. Ecol. Biogeogr.* 2013; 22(3):302–17.
31. Tarkhnishvili D, Gavashelishvili A, Mumladze L. Palaeoclimatic models help to understand current distribution of Caucasian forest species. *Biol. J. Linn. Soc.* 2012; 105(1):231–48.
32. Ülker ED, Tavşanoğlu Ç, Perктаş U. Ecological niche modelling of pedunculate oak (*Quercus robur*) supports the 'expansion–contraction' model of Pleistocene biogeography. *Biol. J. Linn. Soc.* 2018; 123(2):338–47.
33. Willis KJ, Van Andel TH. Trees or no trees? The environments of central and eastern Europe during the Last Glaciation. *Quat. Sci. Rev.* 2004; 23(23–24):2369–87.
34. Magri D. Quaternary history of *Fagus us* in the Italian peninsula. *Annali di botanica.* 1998;56.
35. Magri D. Patterns of post-glacial spread and the extent of glacial refugia of European beech (*Fagus sylvatica*). *J. Biogeogr.* 2008; 35(3):450–63.
36. Bradshaw RH, Kito N, Giesecke T. Factors influencing the Holocene history of *Fagus*. *Forest Ecol. Manag.* 2010; 259(11):2204–12.
37. Magri D, Vendramin GG, Comps B, Dupanloup I, Geburek T, Gömöry D, et al. A new scenario for the Quaternary history of European beech populations: palaeobotanical evidence and genetic consequences. *New Phytol.* 2006; 171(1): 199–221. <https://doi.org/10.1111/j.1469-8137.2006.01740.x> PMID: 16771995
38. *Fagus orientalis*—EUFORGEN European forest genetic resources programme [Internet]. 2009 [cited May 2018]. Available from <http://www.euforgen.org/species/fagus-orientalis/>
39. Hijmans RJ, Cameron SE, Parra JL, Jones PG, Jarvis A. Very high resolution interpolated climate surfaces for global land areas. *Int. J. Climatol.* 2005; 25(15):1965–78.
40. Van Vuuren DP, Edmonds J, Kainuma M, Riahi K, Thomson A, Hibbard K, et al. The representative concentration pathways: an overview. *Clim. Change.* 2011; 109(1–2):5.
41. Harris RM, Grose MR, Lee G, Bindoff NL, Porfirio LL, Fox-Hughes P. Climate projections for ecologists. *Wiley Interdiscip. Rev. Clim. Change.* 2014; 5(5):621–37.
42. Dormann CF, Elith J, Bacher S, Buchmann C, Carl G, Carré G, et al. Collinearity: a review of methods to deal with it and a simulation study evaluating their performance. *Ecography.* 2013; 36(1):27–46.
43. Elith J, Graham CH, Anderson RP, Ferrier S, Guisan A, Hijmans RJ, et al. Novel methods improve prediction of species' distributions from occurrence data. *Ecography.* 2006; 29: 129–151.

44. Salamon-Albert É, Lőrincz P, Pauler G, Bartha D, Horváth F. Drought stress distribution responses of continental beech forests at their xeric edge in Central Europe. *Forests*. 2016; 7(12):298.
45. Babst F, Poulter B, Trouet V, Tan K, Neuwirth B, Wilson R, et al. Site-and species-specific responses of forest growth to climate across the European continent. *Glob. Ecol. Biogeogr.* 2013; 22(6):706–17.
46. Pearman PB, Guisan A, Broennimann O, Randin CF. Niche dynamics in space and time. *Trends Ecol. Evol.* 2008; 23(3):149–58. <https://doi.org/10.1016/j.tree.2007.11.005> PMID: 18289716
47. Thuiller W, Lafourcade B, Engler R, Araújo MB. BIOMOD—a platform for ensemble forecasting of species distributions. *Ecography*. 2009; 32(3):369–73.
48. Fielding AH, Bell JF. A review of methods for the assessment of prediction errors in conservation presence/absence models. *Environ. Conserv.* 1997; 24(1):38–49.
49. Pearson RG, Thuiller W, Araújo MB, Martinez-Meyer E, Brotons L, McClean C, et al. Model-based uncertainty in species range prediction. *J. Biogeogr.* 2006; 33(10):1704–11.
50. Pearson RG, Dawson TP, Liu C. Modelling species distributions in Britain: a hierarchical integration of climate and land-cover data. *Ecography*. 2004; 27(3):285–98.
51. Lisitsyna OV, Giesecke T, Hicks S. Exploring pollen percentage threshold values as an indication for the regional presence of major European trees. *Rev. Palaeobot. Palynol.* 2011; 166(3–4):311–24.
52. Gömöry D, Paule L, Vyšný J. Patterns of allozyme variation in western Eurasian *Fagus*. *Bot. J. Linn. Soc.* 2007; 154(2):165–74.
53. Denk T. The taxonomy of *Fagus* in western Eurasia, 1: *Fagus sylvatica* subsp. *orientalis* (= *F. orientalis*). *Feddes Repertorium*. 1999; 110(3-4):177–200.
54. Denk T. The taxonomy of *Fagus* in western Eurasia. 2: *Fagus sylvatica* subsp. *sylvatica*. *Feddes Repertorium*. 1999; 110(5-6):381–412.
55. Gömöry D, Paule L. Reticulate evolution patterns in western-Eurasian beeches. *Bot. Helv.* 2010; 120(1):63–74.
56. Gömöry D, Paule L, Macejovsky V. Phylogeny of beech in western Eurasia as inferred by approximate Bayesian computation. *Acta Soc. Bot. Pol.* 2018; 87(2).
57. Elith J, Phillips SJ, Hastie T, Dudík M, Chee YE, Yates CJ. A statistical explanation of MaxEnt for ecologists. *Divers. Distrib.* 2011; 17(1):43–57.
58. Filipova-Marinova M, Pavlov D, Coolen M, Giosan L. First high-resolution marine palynological stratigraphy of Late Quaternary sediments from the central part of the Bulgarian Black Sea area. *Quat. Int.* 2013; 293:170–83.
59. Filipova-Marinova M, Pavlov D, Giosan L. Multi-proxy records of Holocene palaeoenvironmental changes in the Varna Lake area, western Black Sea coast. *Quat. Int.* 2016; 401:99–108.
60. Atanassova J. Palaeoecological setting of the western Black Sea area during the last 15000 years. *Holocene*. 2005; 15(4):576–84.
61. Margari V, Gibbard PL, Bryant CL, Tzedakis PC. Character of vegetational and environmental changes in southern Europe during the last glacial period; evidence from Lesvos Island, Greece. *Quat. Sci. Rev.* 2009; 28(13–14):1317–39.
62. Mudie PJ, Rochon A, Aksu AE, Gillespie H. Dinoflagellate cysts, freshwater algae and fungal spores as salinity indicators in Late Quaternary cores from Marmara and Black seas. *Mar. Geol.* 2002; 190(1–2):203–31.
63. Mudie PJ, Marret F, Aksu AE, Hiscott RN, Gillespie H. Palynological evidence for climatic change, anthropogenic activity and outflow of Black Sea water during the late Pleistocene and Holocene: centennial-to decadal-scale records from the Black and Marmara Seas. *Quat. Int.* 2007; 167:73–90.
64. Valsecchi V, Goni MF, Londeix L. Vegetation dynamics in the Northeastern Mediterranean region during the past 23 000 yr: insights from a new pollen record from the Sea of Marmara. *Clim. Past.* 2012; 8(6).
65. Van Zeist W., Bottema S. Late Quaternary vegetation of the Near East. *Beih. Tübinger Atlas Vord. Orient, Reihe A (Naturwiss.)*. 1991; 18, 1–156.
66. Shumilovskikh LS, Tarasov P, Arz HW, Fleitmann D, Marret F, Nowaczyk N, et al. Vegetation and environmental dynamics in the southern Black Sea region since 18 kyr BP derived from the marine core 22-GC3. *Palaeogeogr. Palaeoclimatol. Palaeoecol.* 2012; 337:177–93.
67. Shumilovskikh LS, Arz HW, Wegwerth A, Fleitmann D, Marret F, Nowaczyk N, et al. Vegetation and environmental changes in Northern Anatolia between 134 and 119 ka recorded in Black Sea sediments. *Quat. Res.* 2013; 80(3):349–60.
68. Shumilovskikh LS, Fleitmann D, Nowaczyk NR, Behling H, Marret F, Wegwerth A, et al. Orbital and millennial-scale environmental changes between 64 and 25 ka BP recorded in Black Sea sediments. *Clim. Past.* 2013; 9(5).

69. Woldring H, Bottema S. The vegetation history of East-Central Anatolia in relation to archaeology: the Eski Acıgöl pollen evidence compared with the Near Eastern environment. *Palaeohistoria*. 2002;1–34.
70. Wick L, Lemcke G, Sturm M. Evidence of Late glacial and Holocene climatic change and human impact in eastern Anatolia: high-resolution pollen, charcoal, isotopic and geochemical records from the laminated sediments of Lake Van, Turkey. *Holocene*. 2003; 13(5):665–75.
71. Shatilova I, Mchedlishvili N, Rukhadze L, Kvavadze E. The history of the flora and vegetation of Georgia (South Caucasus). Georgian National Museum, Tbilisi. 2011;1–200.
72. Arslanov KA, Dolukhanov PM, Gei NA. Climate, Black Sea levels and human settlements in Caucasus Littoral 50,000–9000 BP. *Quat. Int.* 2007; 167:121–7.
73. Marret F, Bradley LR, Tarasov PE, Ivanova EV, Zenina MA, Murdmaa IO. The Holocene history of the NE Black Sea and surrounding areas: An integrated record of marine and terrestrial palaeoenvironmental change. *Holocene*. 2019; 29(4):648–61.
74. Tarasov PE, Peyron O, Guiot J, Brewer S, Volkova VS, Bezusko LG, et al. Last Glacial Maximum climate of the former Soviet Union and Mongolia reconstructed from pollen and plant macrofossil data. *Clim. Dyn.* 1999; 15(3):227–40.
75. Tarasov PE, Volkova VS, Webb IIIIT, Guiot J, Andreev AA, Bezusko LG, et al. Last Glacial Maximum biomes reconstructed from pollen and plant macrofossil data from northern Eurasia. *J. Biogeogr.* 2000; 27, 609–620.
76. Bottema S. A late Quaternary pollen diagram from Lake Urmia (northwestern Iran). *Rev. Palaeobot. Palynol.* 1986; 47,241–261.
77. Djamali M, de Beaulieu JL., Shah-hosseini M, Andrieu-Ponel V, Ponel P, Amini A, et al. A late Pleistocene long pollen record from Lake Urmia, NW Iran. *Quat. Res.* 2008; 69,413–420.
78. Leroy S, Marret F, Gibert E, Chalié F, Reyss JL, Arpe K. River inflow and salinity changes in the Caspian Sea during the last 5500 years. *Quat. Sci. Rev.* 2007; 26,3359–3383.
79. Leroy SAG, Tudryn A, Chalié F, López-Merino L, Gasse F. From the Allerød to the mid-Holocene: palynological evidence from the south basin of the Caspian Sea. *Quat. Sci. Rev.* 2013; 78, 77–97.
80. Leroy SAG, López-Merino L, Tudryn A, Chalié F, Gasse F. Late Pleistocene and Holocene palaeoenvironments in and around the middle Caspian basin as reconstructed from a deep-sea core. *Quat. Sci. Rev.* 2014; 101,91–110.
81. Shumilovskikh LS, Hopper K, Djamali M, Ponel P, Demory F, Rostek F, et al. Landscape evolution and agrosylvo-pastoral activities on the Gorgan Plain (NE Iran) in the last 6000 years. *Holocene*. 2016; 26,1676–1691.
82. Kislov AV, Panin A, Toropov P. Current status and palaeostages of the Caspian Sea as a potential evaluation tool for climate model simulations. *Quat. Int.* 2014; 345:48–55.
83. Hanspach J, Kühn I, Pompe S, Klotz S. Predictive performance of plant species distribution models depends on species traits. *Perspect. Plant Ecol. Evol. Syst.* 2010; 12(3):219–25.
84. Cutler DR, Edwards TC Jr, Beard KH, Cutler A, Hess KT, Gibson J, et al. Random forests for classification in ecology. *Ecology*. 2007; 88(11):2783–92. <https://doi.org/10.1890/07-0539.1> PMID: 18051647
85. Pearce J, Ferrier S. Evaluating the predictive performance of habitat models developed using logistic regression. *Ecol. Modell.* 2000; 133(3):225–45.
86. Guisan A, Zimmermann NE, Elith J, Graham CH, Phillips S, Peterson AT. What matters for predicting the occurrences of trees: techniques, data, or species' characteristics? *Ecol. Monogr.* 2007; 77(4):615–30.
87. Peel MC, Finlayson BL, McMahon TA. Updated world map of the Köppen-Geiger climate classification. *Hydrology and Earth System Sciences Discussions, European Geosciences Union*. 2007; 4(2):439–473.
88. Mayer H, Aksoy H. *Walder der Türkei (Forests of Turkey)*. Stuttgart. Gustav FV. 1986.
89. Talebi KS, Sajedi T, Pourhashemi M. *Forests of Iran*. In: *A Treasure From the Past, a Hope for the Future* (Vol. 10). Dordrecht, Heidelberg: Springer; 2014.
90. Avcı M. Türkiye'nin Bitki Çeşitliliği ve Coğrafi Açından Değerlendirmesi. In Akkemik Ü. (Ed.), *Türkiye'nin Doğal-Egzotik Ağaç ve Çalılırları*. Ankara: Orman Genel Müdürlüğü Yayınları; 2018;p.311–318.
91. Bartlein PJ, Harrison SP, Brewer S, Connor S, Davis BAS, Gajewski K, et al. Pollen-based continental climate reconstructions at 6 and 21 ka: a global synthesis. *Clim Dyn.* 2011; 37: 775–802.
92. IPCC, 2014: *Climate Change 2014: Synthesis Report*. Contribution of Working Groups I, II and III to the Fifth Assessment Report of the Intergovernmental Panel on Climate Change [Core Writing Team, Pachauri R.K. and Meyer L.A. (eds.)]. IPCC, Geneva, Switzerland, 151 pp.
93. Denk T, Frotzler N, Davitashvili N. Vegetational patterns and distribution of relict taxa in humid temperate forests and wetlands of Georgia (Transcaucasia). *Biol. J. Linn. Soc.* 2001; 72(2):287–332.

94. Saltré F, Saint-Amant R, Gritti ES, Brewer S, Gauchere C, Davis BA, et al. Climate or migration: what limited European beech post-glacial colonization?. *Glob. Ecol. Biogeogr.* 2013; 22(11):1217–27.
95. Kramer K, Degen B, Buschbom J, Hickler T, Thuiller W, Sykes MT, et al. Modelling exploration of the future of European beech (*Fagus sylvatica* L.) under climate change—range, abundance, genetic diversity and adaptive response. *For. Ecol. Manag.* 2010; 259(11):2213–22.
96. Rubel F, Kottek M. Observed and projected climate shifts 1901–2100 depicted by world maps of the Köppen-Geiger climate classification. *Meteorol. Z.* 2010; 19(2):135–41.